ORIGINAL ARTICLE

Eur. J. Anat. 22 (1): 1-15 (2018)

The isolated colonic mucosa: a new substrate for tissue reconstruction. Isolation, decellularization and characterization by immunohistochemistry and electron microscopy

Laura López-Gómez[1], Teresa Núñez-López[2], Gilberto del Rosario-Hernández[2], Pedro Mestres-Ventura[1, 3]

[1]Department of Human Histology and Pathology, Faculty for Health Sciences, University Rey Juan Carlos , Av. de Atenas s/n, E-28922 Alcorcón, Madrid, Spain, [2]Laboratory of Electron Microscopy, Centre for Technical Support (CAT), University Rey Juan Carlos, 28933 Mostoles, Madrid, Spain, [3]Department of Anatomy and Cell Biology, Medical School, Saarland University, 66421 Homburg (Germany)

SUMMARY

This study proposes the use of isolated colonic mucosa as a "scaffold" for cell cultures and potentially for tissue reconstruction. The main goal of this study was to obtain complete decellularization of the specimens while preserving the superficial basement membrane (BM) as a place for cell attachment and growth. This decellularization technique uses a chelating agent in combination with mechanical vibration, followed by detergents and DNase. The grade of decellularization achieved is assessed by counting the number of cell nuclei stained with propidium iodide (PI). BM marker proteins such as collagen IV, laminin and perlecan were detected by immunohistochemistry (ICC). Transmission (TEM) and scanning electron microscopy (SEM) were used to examine the BM ultrastructure and surface topography.

The results show that the protocol used is suitable for rat colonic mucosa. During the process, material of the *lamina lucida (LL)* was partly removed from the BM, whereas the *lamina densa (LD)* seems to have remained unchanged. The BM had become thinner than the control specimens. The nano-topography of the BM surface is characterized by globules of 34-60 nm in diameter. Human fetal fibroblasts were successfully cultured on this substrate confirming that cells can adhere to and grow on this substrate, at least for the particular cell line used. It can be said that the colonic mucosa is an interesting substrate for *in vitro* studies with cells and presumably also for tissue reconstruction.

Key words: Scaffold – Colonic mucosa – Basement membrane – Decellularization – Electron microscopy – Immunohistochemistry

INTRODUCTION

Today "scaffolds" derived of extra-cellular matrix (ECM), also called bio-scaffolds, enjoy wide acceptance in tissue repair and tissue reconstruction, as numerous experimental and clinical studies confirm (Crapo et al., 2011). So far a number of

Corresponding author: Laura López Gómez, PhD. Department of Basic Health Sciences, Faculty of Health Sciences, University Rey Juan Carlos, Av. de Atenas s/n, Alcorcón, Spain. Phone: +34 914888859.
E-mail: laura.lopez.gomez@urjc.es

Submitted: 7 June, 2017. *Accepted:* 28 July, 2017.

organs have been described from which suitable ECM has been obtained after due preparation. The inner surface of hollow organs such as the urinary bladder (Garthwaite et al., 2014), the esophagus (Ozeki et al., 2006), the small intestine (Badylak et al., 1995), and the amnion (Wilshaw et al., 2006) have all already been successfully used for tissue engineering. Other organs such as skin (Yang et al., 2009; Bondioli et al., 2014; Fini, 2012), pericardium (Mirsadraee et al., 2007; Mendoza-Novelo et al., 2011), cornea (Lynch and Ahearne, 2013) as well as the inner surface of blood vessels (Ketchedjian et al., 2005; Grauss et al., 2005) have also been examined for their suitability.

The architecture and composition of bio-scaffolds are organ-specific. Their structural and molecular characteristics can affect the behavior of transplanted cells. Therefore, the selection of the substrate or scaffold is of vital importance in order to obtain tissue which develops the desired characteristics. The examination and development of tissues suitable for tissue engineering has become a vast field of research.

Isolated colonic mucosa has already been proposed as a scaffold for tissue repair (Mestres et al., 2014). However, greater decellularization of the mucosa specimens was required and this is the main objective of the present study.

The antigenicity of scaffolds of biological origin may cause problems when implanted into the animal. Also, in *in vitro* conditions where no immune system is present cellular debris can exert undesired effects on the implanted cells. In this connection, it is thought that decellularization decreases immunogenicity as cellular components are removed (Ozeki et al., 2006).

The tissue decellularization methods can be classified as physical, chemical and enzymatic. These methods are often combined in order to obtain greater decellularization than is the case with the application of only one method. Many decellularization methods contemplated the use of detergents or chelating agents combined with proteolytic enzymes or physical methods (Spurr and Gipson, 1985; McCarthy and Kaye, 1990; Mestres et al., 1991, 2014; Carlson and Carlson, 1991; Rieder et al., 2004; Gilbert et al., 2006; Hopkinson et al., 2008; Lim et al., 2009).

Since any decellularization process will affect the three-dimensional architecture of ECM, the purpose of decellularization protocols is to remove the cellular material while minimizing such adverse effects. The BMs, which constitute a particular ECM compartment, are particularly sensitive to the effect of proteolytic enzymes (Janoff and Zeligs, 1968). Therefore, decellularization by means of enzymatic agents, which might be suitable in the case of certain ECM scaffolds, is not advisable if the BM is to be retained.

The interest in preserving the BM in a scaffold is due to the fact that this formation can influence the migration of adherent cells, their proliferation and cell interactions, for example between epithelia and mesenchyme cells, and that it plays a particular role in the regeneration of epithelia (Böhme et al., 1992; Simon-Assmann et al., 2009). In this connection, BM analogues have repeatedly demonstrated their usefulness in *in vitro* studies on cell differentiation (Kleinman and Martin, 2005), tumor cell growth (Fridman et al., 1991), stem cells (Philp et al., 2005) and angiogenesis assays (Nicosia and Ottinetti, 1990).

The decellularization protocol in this study uses EDTA combined with mechanical vibration, followed by two detergents applied sequentially, one non ionic, namely Triton X-100 and one ionic, SDS. To assess the grade of decellularization, the cell nuclei were counterstained with PI (Riccardi and Nicoletti, 2006). The persistence of BM was assessed by ICC of specific BM proteins such as collagen IV, laminin and perlecan (Timpl, 1996; Mestres et al., 2014) and its thickness and structure by means of TEM (Jensen et al., 1979; Farquhar, 2006; Mestres et al., 2014), whereas its surface nano-topography was investigated using high resolution SEM (Mestres et al., 2014). As chemical decellularization agents and process-induced cellular debris can affect the cells cultured on the scaffold created, it is of importance to confirm their biocompatibility. For this purpose, human fibroblasts were seeded onto scaffolds of colonic mucosa and cultured for several days. This is the first time that isolated colonic mucosa has been implemented in a cell culture study.

MATERIALS AND METHODS

Experimental design

Colon specimens were obtained from 40 adult Wistar rats of both sexes (200-250 gr body weight). The rats were kept and sacrificed according to EU and national regulations for animal experimentation. This project has also been authorized by the Ethic Commission of the University Rey Juan Carlos.

The initial preparation steps with removal of the epithelial cells of the luminal colon surface have already been described (Mestres et al., 2014). Subsequent to this preparation the specimens were treated with Triton X-100, SDS or with a combined application of both detergents and, when necessary, treated with DNase. Finally specimens were thoroughly washed in a physiological solution.

After a comparison of the effects of single and combined application of the detergents, it was concluded that sequential application was the more effective decellularization procedure. The assessment of the effects covered structure, cellular content and substrate capacity for cell cultures.

Isolation of the colonic mucosa

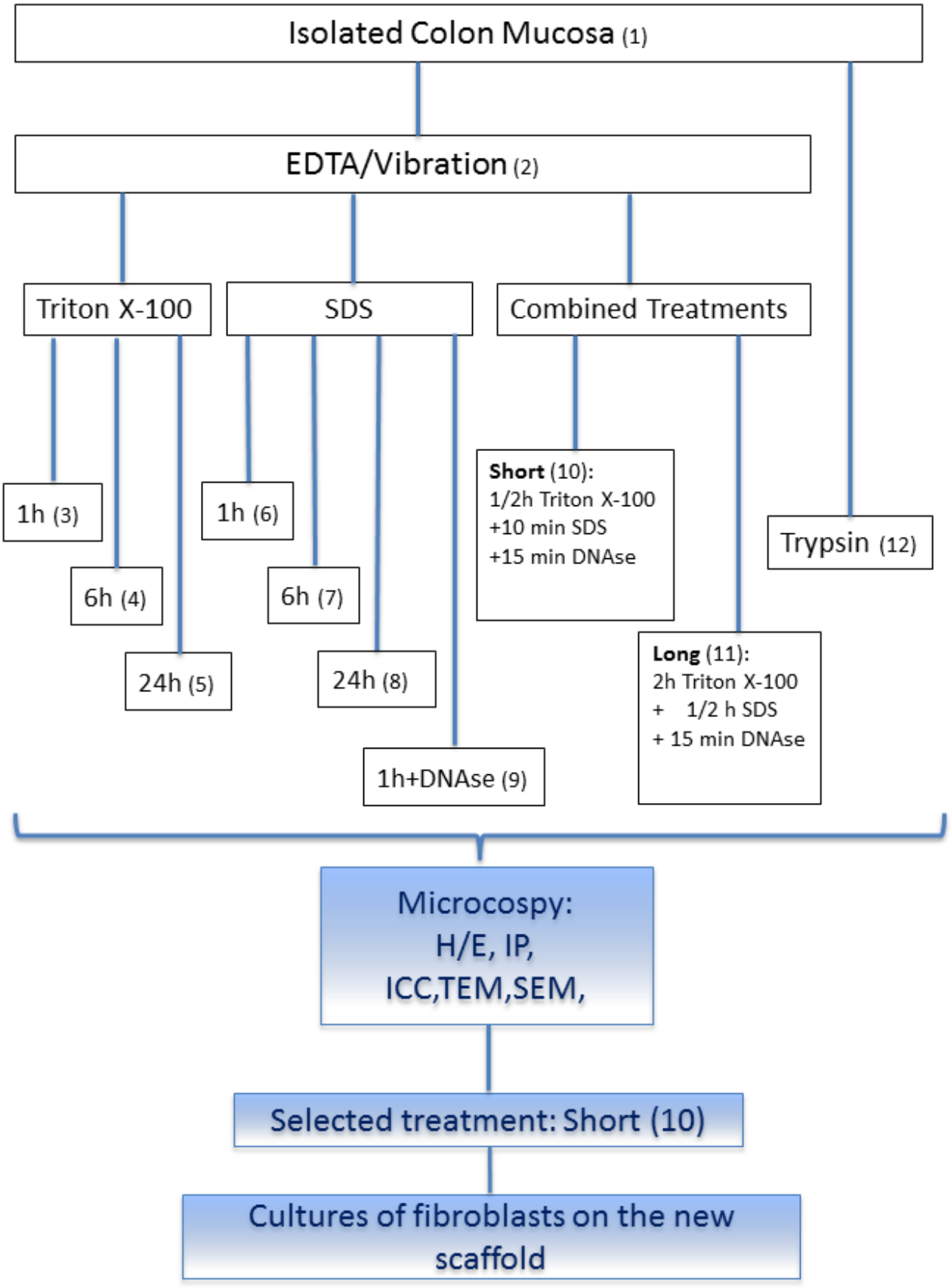

Fig 1. Decellularization procedures used in the present study.

First of all, the rat's colon was removed and washed with 50 ml of Parsons & Paterson solution (1965) at 4°C. A cylindrical rod of 5 mm in diameter was introduced through the lumen of the colon and a circular incision was made at one end to slightly lift the muscular layer and mechanically separate it from the mucosa and submucosa (Andres et al., 1985; Bridges et al., 1986). The tissue left on the rod is mucosa with some attached fragments of submucosa layer. With a lengthwise cut the lining of the colonic lumen can be exposed.

Decellularization

The isolated mucosa sample was divided into several squares of approx. 2 cm side length and attached to plastic holders using the surgical glue Histoacryl (Braun -Aesculap, Germany).

In a first decellularization step the holders with the specimens were plunged into a Parsons & Paterson solution containing 10 mM EDTA at pH 7.4 and without Ca^{2+} and Mg^{2+} for 5 minutes and vibrated (frequency 50 Hz) for 15 seconds. This treatment was repeated for 45 minutes, resulting in the complete removal of surface mucosal epithelium. To restore ion levels the tissue was washed with Parsons & Paterson solution containing Ca^{2+} and Mg^{2+}.

This was the basic material used in all further procedures in the course of this study.

In a second decellularization step two detergents were used: 0.5% Triton X-100 (polyethylene glycol *tert*-octylphenyl ether, Sigma-Aldrich) and SDS 0.5% (sodium dodecylsulphate, Sigma-Aldrich). They were applied separately for different incubation periods (1, 6 and 24 hours) at 4°C with constant rotation. In combination the detergents were applied according to the following time schedules, the most effective being:

Short treatment: Triton X-100 (0.5 %) 30 minutes followed by SDS (0.5%) 10 minutes, and 15 minutes DNase I (Invitrogen).

Long treatment: Triton X-100 (0.5%) 2 hours followed by SDS (0.5%) 30 minutes and 15 minutes DNase I (Invitrogen).

Both combined treatments were performed at 4° C with constant stirring, followed by washing in Parsons & Paterson. The treatment with DNase I (Invitrogen) performed at 37°C was required particularly after SDS treatment in order to remove free-spreading DNA. To eliminate remaining detergent and restore ionic medium, the specimens were washed in Parsons & Paterson solution.

For comparative purposes some specimens were treated with trypsin (Treatment number 12). Samples attached to holders were incubated in 0.25% Trypsin-EDTA (Sigma-Aldrich) in PBS (Dulbecco Phosphate Buffered Saline, Sigma-Aldrich) pH 7.4 for 2h and 24h at 4°C with constant rotation. After treatment samples were washed with Parsons & Paterson solution to remove traces of protease and restore the ionic composition.

The decellularization procedures used in the present study are resumed in Fig. 1.

Evaluation of cellular content

The cellular content of isolated colonic mucosa was determined by three criteria: 1) the non- appearance of cellular nuclear material on hematoxyline and eosin (H/E) stained paraffin sections, 2) no detection of fluorescence of cell nuclei stained with PI and 3) SEM and TEM of decellularized isolated colonic mucosa.

The number of independent experiments, i.e., samples, corresponding to this section (point 1 and 2 of this paragraph) was 27.

Light Microscopy

For light microscopy, decellularized colon samples were fixed with 10% formaldehyde in PBS, dehydrated, embedded in paraffin (Panreac Quimica SA, MP 56-58°C) and 5 µm sections were stained with H/E or PI. The staining of nucleic acids with PI was performed according to the protocol proposed by Molecular Probes (product information 8-11-2003; Riccardi and Nicoletti, 2006).

To determine the persistence of BMs, ICC of specific BM proteins (type IV collagen, laminin, perlecan) was performed. The following antibodies were used: anti-collagen IV (rabbit polyclonal, Abcam, ab6586), anti-laminin (rabbit polyclonal laminin 1 + 2, Abcam, ab7463) and anti-perlecan (rabbit polyclonal, Santa Cruz Biotechnology, H-300).

After de-waxing, the sections were rehydrated and treated with pepsin (Pepsin crystalline, Sigma/ Aldrich, Germany, P6887) to unmask collagen IV and laminin antigens, while for perlecan this pretreatment was unnecessary.

Endogenous peroxidase was inhibited with H_2O_2 for 15 minutes at room temperature, and specific binding sites were blocked with 10% FCS in PBS for 30 minutes in a humid chamber at room temperature.

The primary antibodies against collagen IV (dilution 1/1000), laminin (dilution 1/1500) or perlecan (1/1000 dilution) were incubated overnight in a humidity chamber at 4°C. The binding of the primary antibodies was detected using Histofine Simple N-stain MAX PO (Universal Immune-peroxidase anti-mouse polymer and anti-rabbit; Nichirei Biosciences, Tokyo, Japan). The immune reaction was visualized using the UNIVERSAL VISION MAS kit (Master Diagnostic).

Samples were examined using an Axionplan 2 optical microscope (Zeiss) .The digital images were made with an HCR Axiocam camera (Zeiss) and stored in JPEG and TIFF format.

Electron Microscopy

Samples attached to plastic holders were fixed in 2.5% Glutaraldehyde (Fluka) in buffer cacodylate 0.12 M (Sigma), post-fixed in 1% buffered osmium

tetroxide 2h at 4°C and dehydrated in an increasing alcohol series.

For SEM, the specimens were transferred to 100% acetone and critically point-dried using CO2 as intermediary (Mestres and Rascher, 1981). The samples were sputter-coated with platinum (layer thickness 4-5 nm) (BALC SCD 005 sputter-coater TEC). The examination of the samples was carried out with a Nano-SEM 240 FEG FEI scanning electron microscope, operating at 3-10kV. The number of independent experiments, i.e. samples, corresponding to this section was 28.

For TEM, samples were dehydrated in an ascending alcohol series and embedded in epoxy resin (TAAB resin embedding kit). Ultrathin sections, 80 nm thick and stained for 30 minutes with 1% uranyl acetate (Merck) followed by 20 minutes lead citrate (Reynolds, 1963), were examined at 60 kV in a Jeol JEM 1010 transmission electron microscope, equipped with a Mega View Soft Imaging System III digital camera. The number of independent experiments, i.e., samples, corresponding to this section was 17.

Cell cultures

The BM of the isolated colonic mucosa served as a substrate for primary cultures of human fetal fibroblasts (supplied by Dr. Fernando Serrano Gómez, University Hospital Alcorcón Foundation). For these cultures the isolated mucosa was decellularized using the short treatment procedure.

Before the cells were seeded, the mucosa was incubated in culture medium with antibiotic (DMEM without serum, 1% penicillin / streptomycin) at 4°C and shaken overnight.

Histoacryl® was used to attach the colonic mucosa to a sterile plastic ring (MACROLON®) with the luminal side of the BM facing towards the inside of the ring. The rings were 1 cm high with an inner diameter of 1cm and an outer diameter of 1.2 cm. They were sterilized using ethanol and UV radiation.

The rings with the attached colonic mucosa were placed on a Transwell plate (Falcon- Corning), the membrane of which had been punctured with a sterile needle to facilitate nutrient supply.

Fetal fibroblasts $6x10^4$ were seeded in the central hole of the ring and both ring and Transwell plate were filled with culture medium (DMEM). As the growth of cultured cells on the colonic mucosa cannot be visualized with an inverted microscope, cells were simultaneously cultured on Thermanox® coverslips in order to monitor the growth process.

The cultures were kept in a culture incubator at 37°C and 5% CO2 for 5 to 7 days and the medium was changed every 2 days.

For SEM the samples were fixed with 2.5% glutaraldehyde (Fluka) in 0.12 M cacodylate buffer (Sigma-Aldrich) at pH 7.4 for 1 h at a temperature of 30°C, post-fixed with osmium tetroxide 2% in buffered with Na-cacodylate 0.12 M, washed in buffer, then separated from the rings and prepared for SEM (see section 2.2). Critical point dried specimens were sputter-coated with Au (BALC-TEC SCD 005) and examined under a scanning electron microscope ESEM XL (XL SERIES, PHILIPS).

For correlative SEM/TEM studies selected specimens prepared for SEM were thereafter embedded in epoxy resin as described above. Both, thick (0.5µm) and thin (80 nm) sections were obtained and examined under light- and transmission electron microscope respectively. The number of independent experiments, i.e., samples, corresponding to this section was 8.

Image processing and measurements

Corel PHOTO-PAINT, version 15, was used to improve the brightness and contrast ratio of the SEM and TEM images. The SEM images were analyzed with SPIP software, version 4. The thickness of the BM in the TEM images was measured using the Image J software. To determine the size of the particles, the corresponding images were processed using SCANDIUM (based on analySIS FIVE Soft-Imaging System). As the particles are not perfectly spherical in shape, these are approximate measurements obtained by measuring the diameter of the major axis of the particle. In order to detect and highlight the edges of the BMs in cross section, the filter function of COREL PHOTO PAINT X5 (v 15.2.0.686 (2010) was used.

Statistical analysis.

A descriptive statistical analysis has been performed using Origin Pro 8. The data have been presented as the mean values and included in the text with standard deviation and in relevant cases with percentage error. The total number of independent experiments (samples) is 80.

RESULTS

Histology

The wall of the rat colon is arranged in consecutive concentric layers, from the inside to the outside of the lumen: mucosa, submucosa, muscular and adventitia (Fig. 2 A).

In paraffin sections of samples treated according to the EDTA/vibration and H/E staining protocol, a complete decellularization of the luminal surface and crypts can be observed, leaving the epithelial side of the BM exposed and free of cells (Fig. 2 B).

However, after application of this treatment to the lamina propria, numerous cell nuclei were still present, indicating incomplete decellularization.

Cellular content

The cell nuclei counts are summarized in Figure 3. In untreated samples the number of cell nuclei per area was 232 ± 70 (Fig. 2 E, Fig. 3), whereas, after EDTA / vibration treatment the number of nuclei was reduced by approx. 75%, (Percentage of

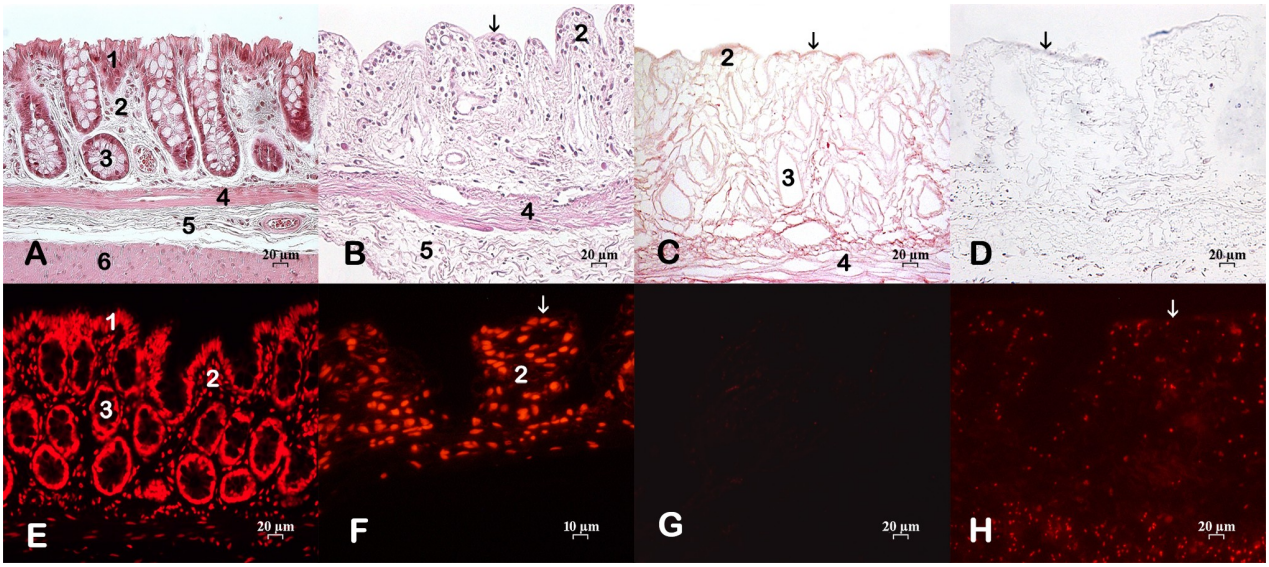

Fig 2. Histology. **A)** Partial view of the colon wall (control). H/E staining. 1: Surface epithelium; 2: Lamina propria; 3: Crypts in cross and length section; 4: Tunica muscularis mucosae; 5: Submucosa with a large blood vessel; 6: Partial view of tunica muscularis. In the following light microscopy images, structural features are indicated as in Fig. 2A. **B)** Isolated colonic mucosa after decellularization after EDTA/vibration treatment. H/E staining. The surface epithelium has been completely removed (arrow). **C)** Isolated colonic mucosa decellularized after the combined treatment (see diagram on figure 1). H/E staining. The surface epithelium has been completely removed (arrow). **D)** Isolated colonic mucosa after trypsin treatment. H/E staining. The surface epithelium has been completely removed (arrow). **E)** Untreated colon wall stained with PI. Note the cell nuclei in red. **F)** Isolated colonic mucosa treated with EDTA/vibration and stained with PI. The surface epithelium has been completely removed (arrow). **G)** Isolated colonic mucosa after combined short treatment (see Fig. 1) and stained with PI. Cell nuclei are no longer visible. **H)** Isolated colonic mucosa after trypsin treatment. Particles stained with PI are still visible and correspond to fragments of cell nuclei trapped in the ECM structure. The surface epithelium has been completely removed (arrow).

Error=4%) which still represents a considerable number of remaining cell nuclei (Fig. 2 F).

In the case of treatment of the isolated colonic mucosa solely with Triton X-100, there was a reduction in the number of cell nuclei of 86% (Percentage of Error=5.7%) compared to the untreated tissue.

There is no correlation between the extent of reduction in the number of cell nuclei caused by Triton X-100 and the action time of the detergent; a similar reduction in cell nuclei numbers was observed in all three time-varying applications (Fig. 3). SDS was more effective, with a reduction rate in the number of nuclei of over 99% (Percentage of Error=15.7%) in comparison with the untreated samples; however this was only reached after a longer exposure time (Fig. 3). The application of SDS followed by DNAse proved to be the most effective procedure, resulting in complete decellularization (Fig. 3).

Furthermore, both short and long exposure treatments, which combined the two above- mentioned detergents with DNase, proved to be successful in decellularizing colon mucosa samples. As it can be seen from a comparison of both treatment procedures that complete decellularization was already achieved with the short-application treatment, it was selected as the method of choice (Figs. 2 C and G, Fig. 3).

In order to hydrolyze the BM and provide a negative control additional experiments were conducted in which isolated colonic mucosa was treated with trypsin. Although trypsin causes decellularization, abundant fragments of cell nuclei still remained trapped in the ECM, which in turn showed remarkable alterations and lost its affinity for histological stains (Figs. 2 D, H and Fig. 3).

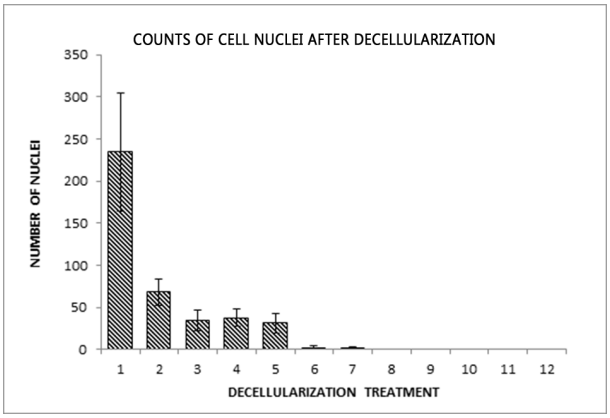

Fig 3. Counts of cell nuclei after decellularization, X= treatments (see graphical abstract in Fig. 1). Y= Counts with standard deviation. (1) 234,2 ± 70,3; (2) 67,6 ± 16; (3) 33,96 ± 12,08; (4) 37,55 ± 10,31; (5) 31,21 ± 11,72; (6) 2,07 ± 2,23; (7) 1,51 ± 1,72; (8) 0; (9) 0; (10) 0; (11) 0; (12) 0.

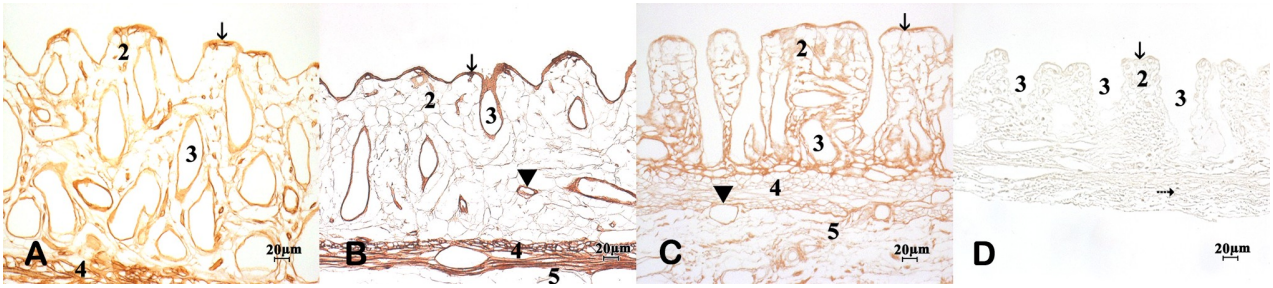

Fig 4. Immunohistochemistry of BM proteins after decellularization in accordance with the combined short treatment. **A)** Collagen IV. The luminal side of the colonic mucosa appears cell free with a sharp line corresponding to the BM (arrow). The BM is also clearly stained at the crypts (3) around blood vessels and smooth muscle of the muscularis mucosae (4); **B)** Laminin. The BM membrane of the surface epithelium (arrow), blood vessels in the lamina propria and in the smooth muscle of lamina muscularis mucosae, are well stained (arrow head). In contrast, the submucosa (5) remains unstained; **C)** Perlecan. The BM membranes are stained but there is also a weak staining of extracellular matrix structures in other regions of the colon wall; **D)** Negative control in which the primary antibody was omitted.

Persistence of basement membrane

ICC showed a normal location pattern for the proteins collagen IV (Fig. 4 A), laminin (Fig. 4B) and perlecan (Fig. 4 C), i.e. the immunoreaction revealed the BMs of surface epithelium and crypts as well as the blood vessels and the muscle cells of the muscular layer of the mucosa. This location pattern applies to all decellularization methods used here, although, in comparison with the control samples, the immunochemical reaction became somewhat weaker with increased treatment duration.

The localization of perlecan immunoreaction differed from that of the other two proteins in as far as it was observed not only at the BMs, but also in the lamina propria and on the meshwork of the submucosa and the muscular layer of the mucosa. The various decellularization protocols applied in this study basically had no effect on the localization pattern of perlecan.

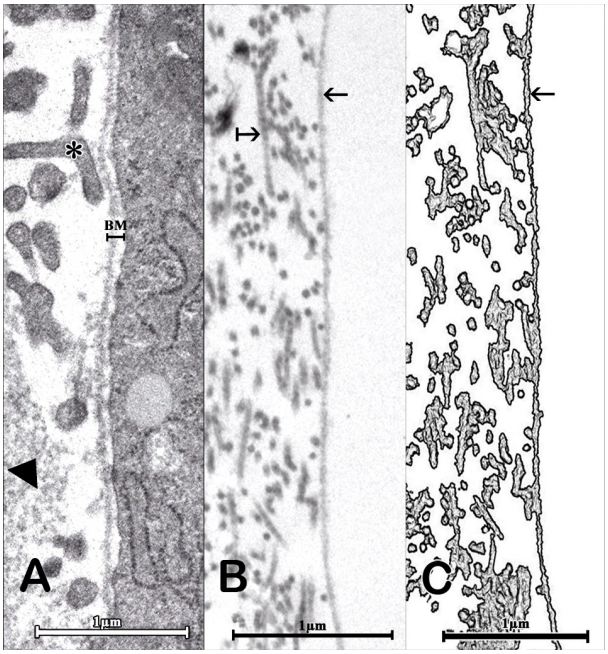

Fig 5. TEM of the colonic mucosa untreated and decellularized. **A)** Colonic mucosa untreated. The basal pole of an enterocyte can be seen in contact with the BM membrane, which shows the characteristic pattern of LL (light) and LD (dark). Below the BM (on left-hand side of picture) thin cell processes (*) and elements of the extracellular matrix (arrow head) of the lamina propria are visible. **B)** Colonic mucosa after cell removal in accordance g with the short combined treatment. The gray line corresponds to the BM membrane of the superficial epithelium (arrow). On the left of the image connective tissue of the lamina propria can be seen. Note the periodicity of collagen micro-fibrils (arrow). **C)** The edges of the BM membranes were digitally enhanced. The arrows mark where the BM membrane thickness was measured.

Thickness of basement membrane

The parameter thickness proved to be very useful as a means of monitoring the effects of the various decellularization methods on the BM. Measurements were taken at locations at which the BM appeared cross-sectioned and the edges were digitally highlighted (Fig. 5 C).

TEM corroborated the ICC findings with regard to the persistence of the BM after the experiments with detergents. Fig. 5 A shows the BM of the superficial epithelium of untreated colon. The characteristic pattern is clearly recognizable: the LL is attached to the basal poles of enterocytes and the LD is in direct contact with the ECM of the lamina propria of the colonic mucosa. While the LL appears bright, the LD presents a greater contrast with a felt-like ultrastructure consisting of very thin filamentous structures (Farquhar, 2006).

Fig. 5 B shows the superficial BM after short combined treatment. The most notable change after this treatment was that LL had disappeared and only LD remained. SEM / TEM correlative microscopy of decellularized specimens confirmed that the LL is no longer present. The metallic layer of SEM coating is deposited directly on the bare BM and does not reveal any clear zone (like an LL) between it and the underlying LD of the BM (Fig. 6

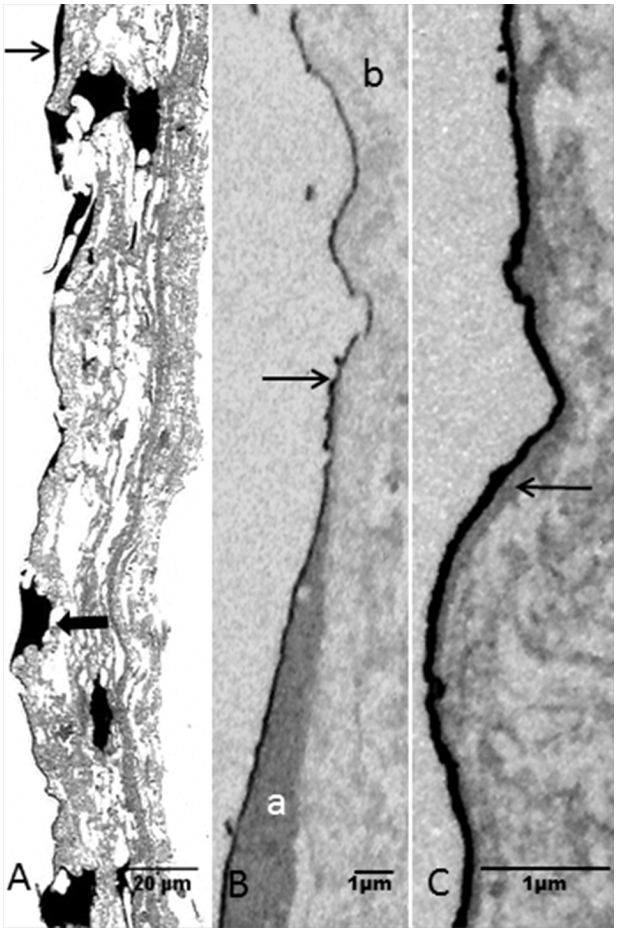

Fig 6. Correlative SEM/TEM microscopy of isolated and decellularized colon mucosa with fibroblasts growing on it. **A)** Thick section stained with toluidine blue. The cells are stained dark. At the surface, very flat cells can be observed (arrow). Some other cells have migrated into deeper layers (thick arrow) and display a stellate shape with thin processes penetrating into the neighboring ECM. **B)** Thin section showing the edge of a fibroblast attached to the BM. The coating appears as a very thin dark layer both on the cell surface and on the parts of the BM which are cell-free. a= cytoplasm at a cell edge or lamellae; arrow= point of transition between cell (left) and cell free BM surface (right); b= lamina propria. **C)** Surface of luminal BM of colonic mucosa coated with Au for SEM. Immediately below the metal layer, a thin gray zone corresponding to BM (arrow) can be distinguished. There is no gap between the coating and the remaining BM.

C).

This observation is evidence of the disappearance of LL.

After decellularization the BM is slightly inhomogeneous, displaying on the free surface a fine irregular edge with a higher density of small particles than in the rest of the membrane. Although similar changes in the BM were observed in all of the decellularization methods used in this study, there were notable differences in the thickness of the BM.

The thickness of the BM was measured in un-

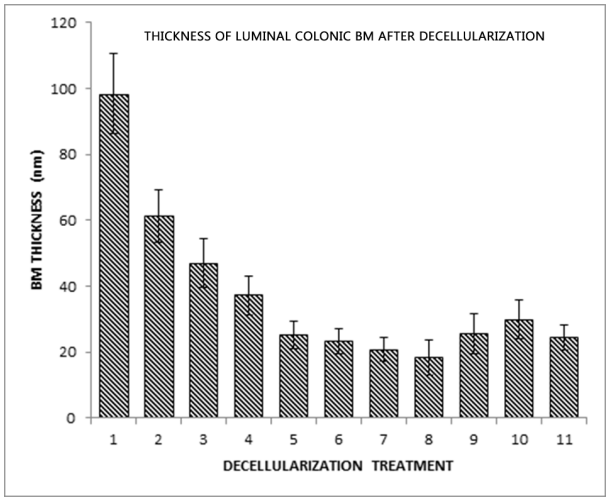

Fig 7. Thickness of luminal colonic BM after decellularization. X= treatments (see graphical abstract in figure 1), Y= BM thickness in nm. Mean values with standard deviation. (1) 98,35 ± 12,1; (2) 61,2 ± 7,99; (3) 47,04 ± 7,34; (4) 37,23 ± 5,84; (5) 25,21 ± 4,23; (6) 23,45 ± 3,83; (7) 20,79 ± 3,67; (8) 18,33 ± 5,17; (9) 25,57 ± 6,16; (10) 29,92 ± 5,78; (11) 24,4 ± 3,75.

treated (control) and in treated specimens and the results are summarized in Fig. 7.

In untreated specimens, the thickness of the BM was approx. 98 nm. At the beginning of our experiments, i.e. after EDTA/vibration treatment, the thickness decreased by approx. 36% (Percentage of Error=1.89%) (Fig. 8 A). Depending on the duration of treatment with Triton X-100 the BM became increasingly thinner (Figs. 8 B, E, H).

SDS appears to have been more aggressive than Triton X-100, resulting in a reduction in thickness of the BM of up to 80% (Percentage of Error=4%) (Figs. 8 C, F, I, and Fig. 7).

The thickness of the BMs after combined treatment with detergents was approx. 25 to 30 nm, i.e. a decrease of approx. 70% (Percentage of Error=2.77%), in particular after the short-time protocol (Figs. 8 D,G and Fig. 7).

The BM was no longer visible in TEM images after treatment with trypsin, i.e. it had disappeared (not shown).

Nano-topography of the basement membrane surface

The SEM image of the decellularized colon luminal surface shows smooth areas, especially between the abundant mouths of the crypts (Fig. 9 A). These smooth areas correspond to the superficial BM. Crypts appear cell-free as well, showing a surface pattern reminiscent of the folds of a bellows, probably due to a certain flattening of the sample at some point in the preparation.

At higher magnifications the surface of the BM is characterized by the presence of small globules with a diameter varying between 30-45 nm (Figs. 9 B, C and Fig.10).

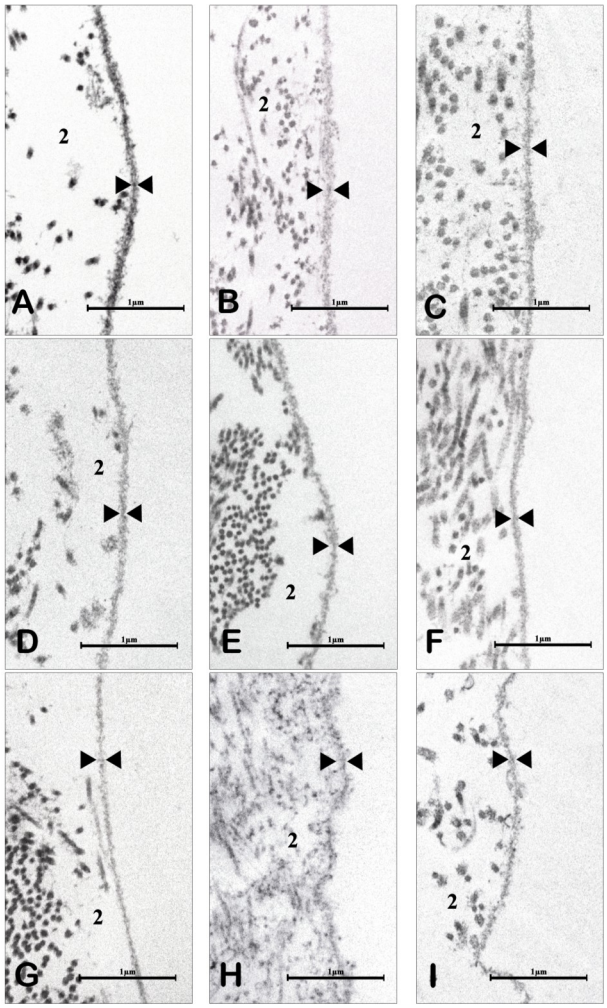

Fig 8. TEM of the BM membrane of the superficial epithelium of the colonic mucosa after decellularization in accordance with the methods used in this study. Arrowheads mark the edges of the BM membranes. Differences in thickness in the BM membrane were not apparent to the naked eye, although there were slight changes in the density of the same depending on the treatment applied. **A)** EDTA/Vibration treatment. **B)** EDTA/Vibration/1h Triton X-100. **C)** EDTA/Vibration/1h SDS. **D)** Combined treatment (long-term). **E)** EDTA/Vibration/6h Triton X-100. **F)** EDTA/Vibration/6h SDS. **G)** Combined treatment (short-term). **H)** EDTA/Vibration/24h Triton X-100. **I)** EDTA/Vibration/24h SDS.

As shown in Fig. 9C, the globules are small spheres with small openings or pores between them of a diameter of 20 nm or more. The globules are widely distributed throughout the surface of the BM, like a surface covered with gravel. Sometimes the globules have formed aggregates that almost overpower the membrane, but also often appear embedded in the membrane itself.

It is remarkable that, regardless of the treatment applied, the size of the globules is similar in all cases. The average diameters of the globules in each decellularization treatment procedure are summarized in Fig. 10.

In particular after SDS treatment a network of filaments covering the sample was observed (Fig. 9 D). Such fibrillary networks were observed only in specimens treated with SDS and proved to be highly sensitive to DNase.

Experiments with trypsin served to demonstrate the enzymatic degradation of the BM, possibly providing an interesting substrate for cell cultures. Histological sections stained with H/E (Fig. 2 D) showed that, after a 24-hour treatment with trypsin, the BM had disappeared completely. Accordingly, ICC of the three BM-proteins, collagen IV, laminin and perlecan, returned negative results.

SEM observations confirmed the effects of trypsin on the BM, which was completely hydrolyzed, exposing the underlying connective tissue, where collagen bundles of the lamina propria could easily be recognized (Figs. 9 E, F).

Cell cultures

Although it had been decellularized, the optical qualities of the isolated colonic mucosa were poor. This was due mainly to the thickness of these specimens, which impeded microscopic monitoring of the evolution of the cell cultures.

Parallel fibroblast cultures on Thermanox ® coverslips showed that approx. 4 hours after seeding, the cells had adhered and, a further 24 hours later, had begun to change their form into an elongated shape (Figs. 11 A, B). Although the imaging of cultures on the BM was very limited with the invert microscope, it was possible to ascertain a similar timing with regard to cell behavior (adhesion, elongation and migration) as observed with Thermanox®. Moreover, our observations confirm the ability of these cultures to proliferate in a normal way, achieving confluence after 5-7 days of cultivation. At this stage the cells displayed a flattened and elongated shape, forming a carpet, which covered the BM and the mouths of the crypts (Fig. 11 C). In addition to these areas with flattened cells, other cells were observed which appeared round in shape, with numerous microvilli at the surface, forming pairs resembling young post-mitotic cells. The presence of lamellipodia and filopodia is an expression of cell membrane activity and such surface profiles correlate well with the phenotype of fibroblasts (Fig. 11 D).

Correlative SEM/TEM electron microscopy has shown that, as seen in thick sections, the fibroblasts located on the surface were extremely flat and closely adhered to the substrate, in this case the BM, covered by a thin gold layer required for SEM (Fig. 6 A). In thick sections it was possible to see the deep layers of the sample, where many cells with numerous extensions make contact with the tissue, in that case the ECM of the mucosa (Fig. 6 A). In thin sections the metal coating covers both the bare BM and the flat surface cells (Fig. 6 B). This metal coating lies directly on the BM (Fig. 6 C) and on the upper cell membrane of the fibro-

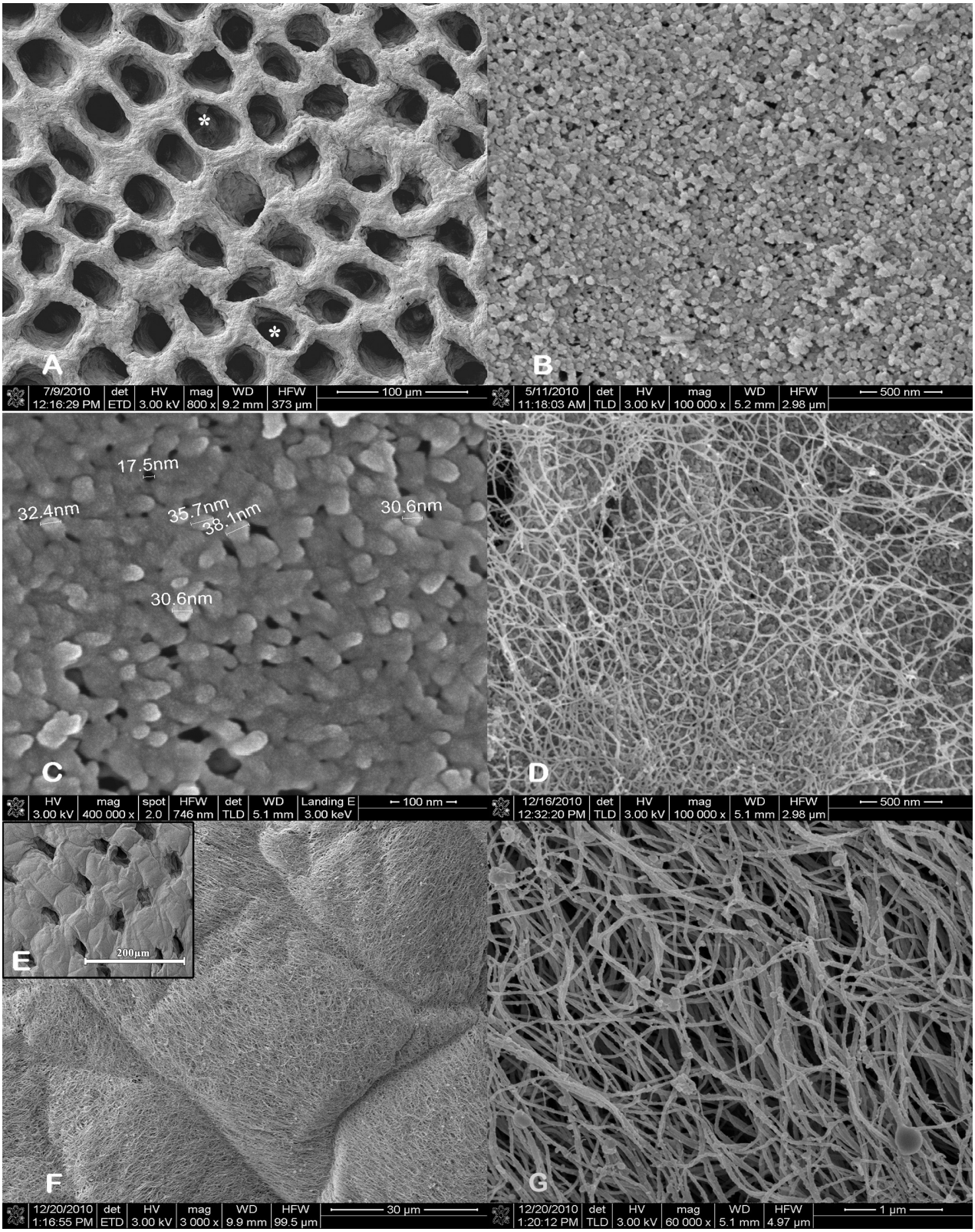

Fig 9. SEM of the luminal surface of the colonic mucosa after decellularization. **A)** Overview showing the cell-free BM surface and the mouths of the crypts (*). **B)** Epithelial side of the BM membrane at higher magnification. Note the presence of globules. **C)** Measurements of particle diameter or globules. Some globules rise to the surface, whereas others appear embedded in the BM membrane. **D)** Surface of the BM membrane after SDS treatment. Note the presence of a network of fibers which subsequently disappeared upon the application of the enzyme DNase. **E)** Insert showing the surface of the mucosa after trypsin treatment. Note the regular distribution of the crypts (dark mouth). **F)** The enzymatic action of trypsin has hydrolyzed the BM membrane rendering the collagen fibers underneath directly visible. **G)** Detail of Fig. 9F. The collagen fibers do not appear to have been affected by the action of trypsin, indicating that only the BM has been removed.

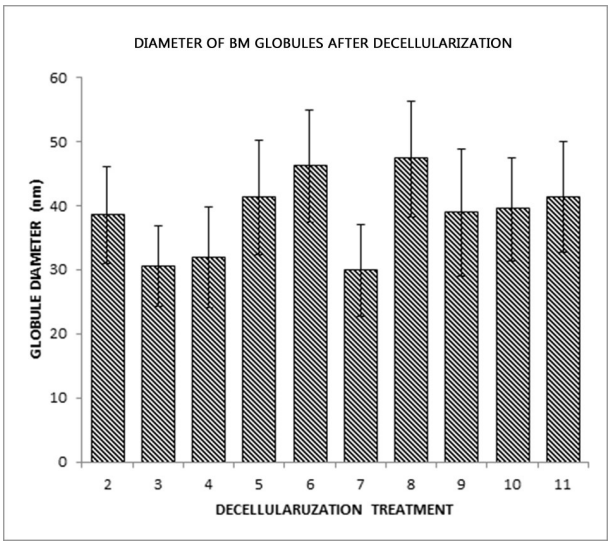

Fig 10. Diameter of BM globules after decellularization. X= treatments (see graphical abstract). Y= Diameter of globules in nm with standard deviation. (2) 38,5 ± 7,5; (3) 30,5 ± 6,3; (4) 31,9 ± 7,8; (5) 41,2 ± 8,9; (6) 46,2 ± 8,7; (7) 29,8 ± 7,2; (8) 47,3 ± 9; (9) 38,9 ± 9,9; (10) 41,3 ± 8,6; (11) 39,4 ± 8,1.

blasts (Fig. 6 B) while underneath, the fibroblasts appear to be tightly attached to the substrate, i.e. BM (Fig. 6 B).

DISCUSSION

The present study has shown for the first time that rat colon mucosa can be used as a substrate for cell cultures, thus adding it to the long list of bio -scaffolds derived from hollow organs.

The protocol developed for this purpose uses a chelating agent (EDTA) and two detergents, namely Triton X-100 and SDS. This procedure permits complete decellularization of the specimen while, at the same time, preserving the luminal BM. It differs from other procedures in which detergents are applied alone or in combination, for example, with hypo- and hyper-osmotic factors and proteolytic enzymes (Liao et al., 2007; Du and Wu, 2011; Soto-Gutierrez et al., 2011; Keane et al., 2013; Friedrich et al., 2014). In studies, which did use a combination of the same detergents, the detergents were more highly concentrated and the treatment was of longer duration than in our study

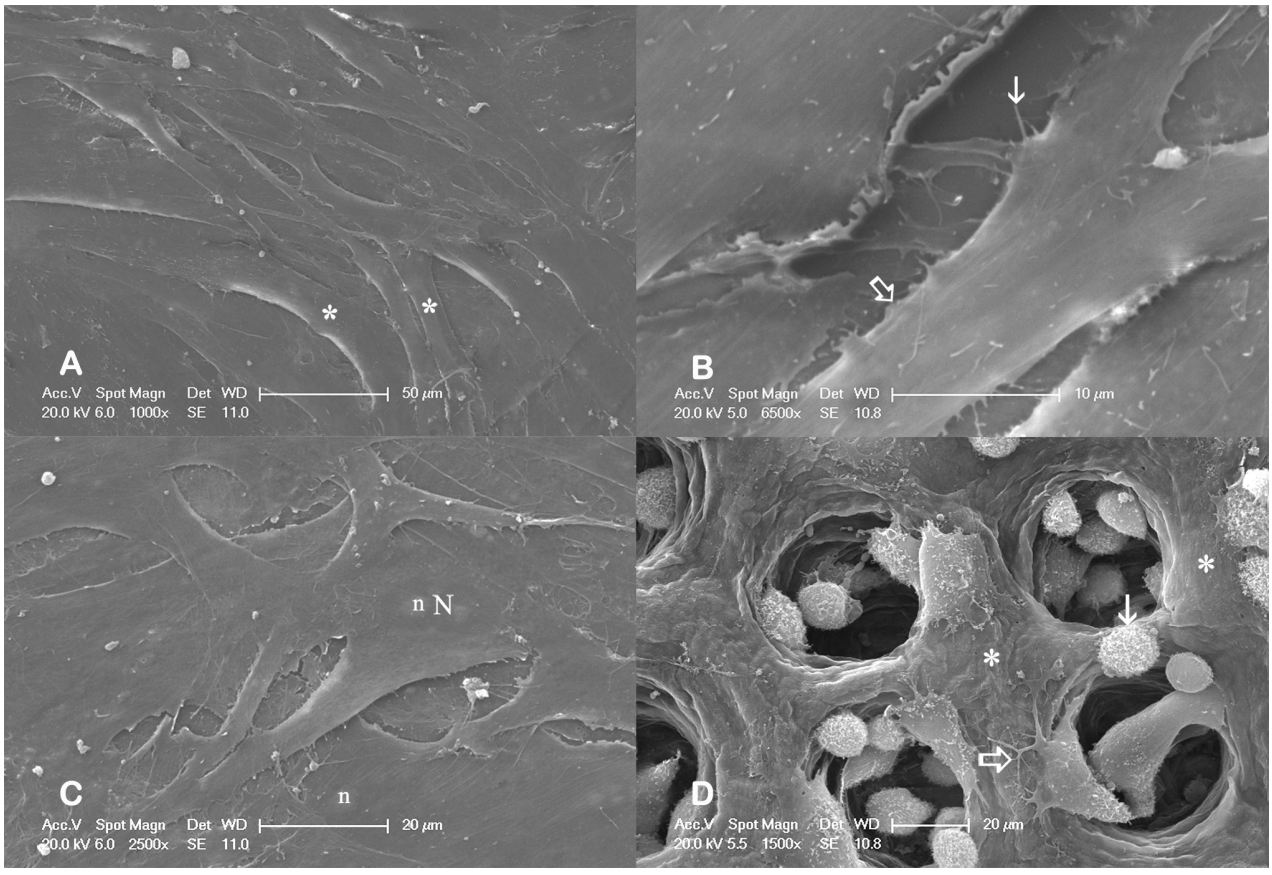

Fig 11. SEM of fetal human fibroblasts cultures. **A)** Cultures on Thermanox® coverslips. The arrangement of the cells with interconnected elongated forms (*) resembles that of a swarm of fish. **B)** Cultures on Thermanox® coverslips. At higher magnifications, very characteristic surface profiles can be observed, such as filopodia of varying length (arrow) as well as ruffled borders (thick arrows). **C)** Cultures on BM of decellularized colon mucosa. The cells show the same arrangement pattern as described above. Note the presence of a cell nucleus (N) with its nucleoli (n), rising up below the plasma membrane. **D)** Detail of a culture similar to the previous one (Fig. 11C). Area with low cell density in which the surface of the BM membrane (*) can be seen. Round cells with numerous microvilli (arrow) are visible, probably related with cell division. The cells appear to be well attached to the substrate and show branched processes (thick arrow).

(Rieder et al., 2004; Hudson et al., 2004). In our study the application period of each agent was reduced, thus minimizing damage to the ECM and particularly to the BM.

In order to determine the degree of decellularization a well-established procedure was selected, namely the staining of nucleic acids with fluorescent dyes and H/E (Crapo et al., 2011). DNase treatment was used to remove remaining DNA from the surfaces and tissue structure (Narayanan et al., 2009; Keane et al., 2013).

The BM constitutes a specific compartment of the ECM, located between parenchymal cells and connective tissue (Brown et al., 2006). Its thickness is a parameter of considerable value in the assessment of their status under both normal and pathological conditions. Using this parameter differences in the thickness of the BM were detected in various organs of the rat (Osawa et al., 1984), as well as modifications thereof with regard to the process of reproduction and embryonic development (Dockery et al., 1998). This parameter is widely applied in the field of experimental pathology and medical diagnostics, for instance, in renal pathology (Dische, 1992; Das et al., 1996), in inflammatory diseases of the colon (Gledhill et al., 1984) and diabetes (Williamson et al., 1969; Carlson et al., 2003).

When measuring the thickness of the BM certain features such as precise determination of the edges of the BM and the cutting plane need to be taken into account (Wu et al., 2010).

Generally in TEM images, the edges of a BM are well defined by the staining of the structure with heavy metals (Farquhar, 2006). We implemented digital image processing in our study in order to define the edges of the BMs with greater precision (Carlson et al., 2003; Rangayyan et al., 2010). The proper orientation of the specimens in the block during embedding proved to be decisive in the minimization of errors with regard to the cutting plane. Moreover, in our TEM images, zones in which the BM had been cut obliquely could be easily recognized with the help of neighboring structures.

Our results indicate that the decellularization procedures used in the present study cause alterations in the structure of the BM, resulting in a manifest thinning of this compartment of the ECM. These changes can be attributed to the action mechanisms of the agents, EDTA and also to those of both detergents (Stanley et al., 2003; Yurchenco, 2011; Faulk et al., 2014).

The effects of EDTA on the superficial BM of colon have been already reported on in a previous study (Mestres et al., 2014). In the present study, new evidence for the loss of LL was obtained using correlative SEM / TEM microscopy. The effects of both detergents, Triton X-100 and SDS, take place mostly in the LL, mimicking those described for EDTA. Both detergents are able to solubilize proteins and other tissue components (Cebotari et al., 2010). We can confirm the reports of other authors that the observed effects of SDS were more intense than those of Triton X-100 (Bhuyan et al., 2010; Faulk et al., 2014). The reduction in thickness of the BM is a phenomenon closely associated with the treatment applied in our experiments and is definitely due to the extraction processes exerted by the decellularizing agents (Patel et al., 2008; Faulk et al., 2014).

Recent studies on the distribution of specific BM proteins have shown that some of the proteins, for example laminin, appear to be unevenly distributed and are mostly located in the LL (see Menter and Dubois, 2012, page 6, Fig. 3). This is also supported by the fact that, after standard tissue preparation for electron microscopy, the BM displays two clearly visible layers or sheets, the LL and the LD (Farquhar, 2006). Although tissue preparation with cryo- techniques reveals a structurally homogenous BM, this does not exclude the existence at molecular level of an unequal distribution of specific molecules, with differences between ad- epithelial and ab-epithelial sides of the BM. The ad-epithelial side of the BM could be less stable than the ab-epithelial, because in the former the links with the epithelial cells seem to be easier to break than those of the LD with the underlying ECM. Nonetheless, after decellularization and although the LL had completely disappeared, all three marker proteins were detected in the remaining BM. As it would seem that all three marker proteins are distributed throughout the BM, the BM layout in the *laminae* might be dependent on other molecular and / or structural parameters.

Cells react to topographical features of the substrate (ridges, sulci, protrusions different sizes etc.) with remarkable changes in metabolism, in cell alignment and orientation, motility, adhesion and cell shape (Folkman and Moscona, 1978; Curtis and Wilkinson, 1999; Kim et al., 2012).

The nanotopography of the BM surface, as seen with SEM, is characterized by the presence of very small globules, which are all similar in size, regardless of the decellularization treatment applied. This seems to relate to the basic structure of BM (Carlson and Carlson, 1991; Mestres et al., 2014).

Typical surface formations of BMs of the digestive tract are so-called "fenestrae". These formations are mostly related to the passage of cells through the BM, but under the influence of mechanical stimuli their number can increase (Mestres et al., 1991). The agents applied in decellularization experiments can cause significant extraction of materials from the BM, which renders this structure weak and unstable. The decellularization protocol used in this study was configured to ensure that, despite reduction in the thickness of the BM layer, such a degree of structural weakness was not reached.

Stiffness and mechanical properties can also influence the behavior of cells. However, although

the isolated colonic mucosa is rather thin and not very rigid, these weaknesses can be compensated by the fixation of the isolated mucosa to the Makrolon® rings. In view of the fact that the fibroblasts grown thereon display completely normal growth and pattern formation (Emonard et al., 1987; Kleinman and Martin, 2005), the new scaffold can be considered biocompatible.

The question of biocompatibility is important in several respects. First of all, the chemicals used for decellularization have to be washed out of the tissue as retention in the tissue structure can exert undesired effects on the cells cultured on the scaffold (Crapo et al., 2011; Friedrich et al., 2014). Secondly, it is important to remember that in primary or cell line cultures, many products, particularly bioactive substances such as growth factors located in the BM (sponge effect), can be washed out in the decellularization process. They are then not available to the cells for growth and may, possibly, have to be replaced (Reing et al., 2010). Serum, as a standard culture medium, was added to our fibroblast cultures. Further studies with this protocol are already underway to determine whether this new scaffold can also be implemented to culture other cell types and cell lines.

Conclusions

The goal of this study was to establish a method by which to decellularize the isolated mucosa of the colon while, at the same time, ensuring optimal preservation of the BM.

The strategy chosen, namely the use of quelants, two detergents applied sequentially and DNase, produced the desired results: the BM is preserved to a large extent and the mucosa ECM retains sufficient mechanical stability to enable the obtaining of cell cultures.

The sequential combination of two detergents has proved to be greatly superior to the use of hydrolytic enzymes as these have a severe effect on the structure and on the mechanical and probably also on the chemical properties of the specimen.

In order to determine the biocompatibility of this substrate, human fibroblasts were cultured on it. These cells showed a normal behavior (morphological appearance, substrate adhesion, and migration with formation of a cell layer on the surface as well as penetration inside the substrate), comparable in all respects to that which they present when grown on current substrates for cell cultures (Emonard et al., 1987). Thus, the hypothesis that cells can adhere to and grow on this substrate has been confirmed, at least for the particular cell line used.

In conclusion, it can be said that the colonic mucosa is an interesting substrate for *in vitro* studies with cells and presumably also for tissue reconstruction.

Competing interests

The authors declared that they have not competing interest.

ACKNOWLEDGEMENTS

We thank Prof. Dr. K. H. Schaefer (Polytechnic University Kaiserslautern) for critical reading of the manuscript. We also thank to Raquel Franco, Julio Paredes and Antonio Marquez (Department of Histology and Pathology, URJC) and Roberto Castro (Electron Microscopy Laboratory, CAT, URJC) for technical assistance. We especially thank Dr. Esperanza Perez and Dr. Laureano Cuevas (Laboratory for Electron Microscopy, Instituto Carlos III, Majadahonda) for advice and assistance in several respects. For the linguistic revision of the manuscript we thank Mrs. Ann Soether.

This research has received generous support from Saarland University (to P.M.) and from the Multimate-Challenge Project funded by the Madrid Region under program S2013/MIT-2862 (to G. del R.)

REFERENCES

ANDRES H, BOCK R, BRIDGES RJ, RUMMEL W, SCHREINER J (1985) Submucosal plexus and electrolyte transport across rat colonic mucosa. *J Physiol*, 364: 301-312.

BADYLAK SF, TULLIUS R, KOKINI K, SHELBOURNE KD, KLOOTWYK T, VOYTIK SL, KRAINE MR, SIMMONS C (1995) The use of xenogeneic small intestinal submucosa as a biomaterial for Achilles tendon repair in a dog model. *J Biomed Mater Res*, 29(8): 977-985.

BHUYAN AK (2010) On the mechanism of SDS-induced protein denaturation. *Biopolymers*, 93(2): 186-199.

BÖHME M, DIENER M, MESTRES P, RUMMEL W (1992) Direct and indirect actions of $HgCl_2$ and methyl mercury chloride on permeability and chloride secretion across the rat colonic mucosa. *Toxicol Appl Pharmacol*, 114(2): 285-294.

BONDIOLI E, FINI M, VERONESI F, GIAVARESI G, TSCHON M, CENACCHI G, MELANDRI D (2014) Development and evaluation of a decellularized membrane from human dermis. *J Tissue Eng Regen Med*, 8 (4): 325-336.

BRIDGES RJ, RACK M, RUMMEL W, SCHREINER J (1986) Mucosal plexus and electrolyte transport across the rat colonic mucosa. *J Physiol*, 376: 531-542.

BROWN B, LINDBERG K, REING J, STOLZ DB, BADYLAK SF (2006) The basement membrane component of biologic scaffolds derived from extracellular matrix. *Tissue eng*, 12(3): 519-526.

CARLSON EC, CARLSON BM (1991) A method for preparing skeletal-muscle fiber basal laminae. *Anat Rec*, 230(3): 325-331.

CARLSON EC, AUDETTE JL, VEITENHEIMER NJ, RISAN JA, LATURNUS DI, EPSTEIN PN (2003) Ultrastructural morphometry of capillary basement mem-

brane thickness in normal and transgenic diabetic mice. *Anat Rec A Discov Mol Cell Evol Biol*, 271(2): 332-341.

CEBOTARI S, TUDORACHE I, JAEKEL T, HILFIKER A, DORFMAN S, TERNES W, LICHTENBERG A (2010) Detergent decellularization of heart valves for tissue engineering: toxicological effects of residualdetergents on human endothelial cells. *Artif Organs*, 34(3): 206-210.

CRAPO PM, GILBERT TW, BADYLAK SF (2011) An overview of tissue and whole organ decellularization processes. *Biomaterials*, 32(12): 3233-3243.

CURTIS A, WILKINSON C (1998) New depths in cell behaviour: reactions of cells to nanotopography. *Biochem Soc Symp*, 65: 15-26.

DAS AK, PICKETT TM, TUNGEKAR MF (1996) Glomerular basement membrane thickness - a comparison of two methods of measurement in patients with unexplained haematuria. *Nephrol Dial Transplant*, 11(7): 1256-1260.

DISCHE FE (1992) Measurement of glomerular basement membrane thickness and its application to the diagnosis of thin-membrane nephropathy. *Arch Pathol Lab Med*, 116(1): 43-49.

DOCKERY P, KHALID J, SARANI SA, BULUT HE, WARREN MA, LI TC, COOKE D (1998) Changes in basement membrane thickness in the human endometrium during the luteal phase of the menstrual cycle. *Hum Reprod Update*, 4(5): 486-495.

DU L, WU X (2011) Development and characterization of a full-thickness acellular porcine cornea matrix for tissue engineering. *Artif Organs*, 35(7): 691-705.

EMONARD H, CALLE A, GRIMAUD JA, PEYROL S, CASTRONOVO V, NOEL A, LAPIÈRE CM, KLEINMAN HK, FOIDART JM (1987) Interactions between fibroblasts and a reconstituted basement membrane matrix. *J Invest Dermatol*, 89: 156-163.

FARQUHAR MG (2006) The glomerular basement membrane: not gone, just forgotten. *J Clin Invest*, 116 (8): 2090-2093.

FAULK DM, CARRUTHERS CA, WARNER HJ, KRAMER CR, REING JE, ZHANG L, D´AMORE A, BADYLACK SF (2014) The effect of detergents on the basement membrane complex of a biologic scaffold material. *Acta Biomater*, 10(1): 183-193.

FINI M, BONDIOLI E, CASTAGNA A, TORRICELLI P, GIAVARESI G, ROTINI R,MELANDRI D (2012) Decellularized human dermis to treat massive rotator cuff tears: in vitro evaluations. *Connect Tissue Res*, 53(4): 298-306.

FOLKMAN J, MOSCONA A (1978) Role of cell shape in growth control. *Nature*, 273: 345-349.

FRIDMAN R, KIBBEY MC, ROYCE LS, ZAIN M, SWEENEY M, JICHA DL, YANNELLI JR, MARTIN GR, KLEINMAN HK (1991) Enhanced tumor growth of both primary and established human and murine tumor cells in athymic mice after coinjection with Matrigel. *J Natl Cancer Inst*, 83(11): 769-774.

FRIEDRICH LH, JUNGEBLUTH P, SJÖQVIST S, LUNDIN V, HAAG JC, LEMON G, GUSTAFSSON Y, AJALLOUEIAN F, SOTNICHENKO A, KIELSTEIN H, BURGUILLOS MA, JOSEPH B, TEIXEIRA AI, LIM ML, MACCHIARINI P (2014) Preservation of aortic root architecture and properties using a detergent-enzymatic perfusion protocol. *Biomaterials*, 35(6): 1907-1913.

GARTHWAITE M, HINLEY J, CROSS W, WARWICK RM, AMBROSE A, HARDAKER H, EARDLEY I, SOUTHGATE J (2014) Use of donor bladder tissues for in vitro research. *BJU Int*, 113(1): 160-166.

GLEDHILL A, COLE FM (1984) Significance of basement membrane thickening in the human colon. *Gut*, 25(10): 1085-1088.

GILBERT TW, SELLARO TL, BADYLAK SF (2006) Decellularization of tissues and organs. *Biomaterials*, 27 (19): 3675-3683.

GRAUSS RW, HAZEKAMP MG, OPPENHUIZEN F, VAN MUNSTEREN CJ, GITTENBERGER-DE GROOT AC, DE RUITER MC (2005) Histological evaluation of decellularised porcine aortic valves: matrix changes due to different decellularisation methods. *Eur J Cardiothorac Surg*, 27(4): 566-571.

HOPKINSON A, SHANMUGANATHAN VA, GRAY T, YEUNG AM, LOEWE J, JAMES DK, DUA HS (2008) Optimization of amniotic membrane (AM) denuding for tissue engineering. *Tissue Eng Part C Methods*, 14(4): 371-381.

HUDSON TW, ZAWKO S, DEISTER C, LUNDY S, HU CY, LEE K, SCHMIDT CE (2004) Optimized acellular nerve graft is immunologically tolerated and supports regeneration. *Tissue Eng*, 10(11-12): 1641-1651.

JANOFF A, ZELIGS JD (1968) Vascular injury and lysis of basement membrane in vitro by neutral protease of human leukocytes. *Science*, 161(3842): 702-704.

JENSEN EB, GUNDERSEN HJG, ØSTERBY R (1979) Determination ofmembrane thickness distribution from orthogonal intercepts. *J Microsc,* 115(1): 19-33.

KEANE TJ, LONDONO R, CAREY RM, CARRUTHERS CA, REING JE, DEARTH CL, D'AMORE A, MEDBERRY CJ, BADYLAK SF (2013) Preparation and characterization of a biologic scaffold from esophageal mucosa. *Biomaterials*, 34(28): 6729-6737.

KETCHEDJIAN A, JONES AL, KRUEGER P, ROBINSON E, CROUCH K, WOLFINBARGER L Jr, HOPKINS R (2005) Recellularization of decellularized allograft scaffolds in ovine great vessel reconstructions. *Ann Thorac Surg*, 79(3): 888-896.

KIM DH, PROVENZANO PP, SMITH CL, LEVCHENKO A (2012) Matrix nanotopography as a regulator of cell function. *J Cell Biol*, 197(3): 351-360.

KLEINMAN HK, MARTIN GR (2005) Matrigel: basement membrane matrix with biological activity. *Sem Cancer Biol*, 15 (5): 378-386.

LIAO J, JOYCE EM, SACKS MS (2007) Effects of decellularization on the mechanical and structural properties of the porcine aortic valve leaflet. *Biomaterials*, 29(8): 1065-1074.

LIM LS, RIAU A, POH R, TAN DT, BEUERMAN RW, MEHTA JS (2009) Effect of dispase denudation on amniotic membrane. *Mol Vis*, 15: 1962-1970.

LYNCH AP, AHEARNE M (2013) Strategies for develop-

ing decellularized corneal scaffolds. *Exp Eye Res*, 108: 42-47.

MCCARTHY KJ, KAYE GI (1990) Comparison of osmium/sonication and EDTA/sonication microdissection techniques in exposing the epithelial basal lamina surface of developing rat colon. *J Electron Microsc Tech*, 14(4): 367-372.

MENDOZA-NOVELO B, ÁVILA EE, CAUICH-RODRÍGUEZ JV, JORGE-HERRERO E, ROJO FJ, GUINEA GV, MATA-MATA JL (2011) Decellularization of pericardial tissue and its impact on tensile viscoelasticity and glycosaminoglycan content. *Acta Biomater*, 7(3): 1241-1248.

MENTER DG, DUBOIS RN (2012) Prostaglandins in cancer cell adhesion, migration, and invasion. *Int J Cell Biol*, Article ID 723419, 21 pages.

MESTRES P, RASCHER K (1981) Supraependymal cell clusters in the rat brain. *Cell Tissue Res*, 218: 41-58.

MESTRES P, DIENER M, MAI H, RUMMEL W (1991) The epithelial basal lamina of the isolated colonic mucosa. Scanning and transmission electron-microscopy. *Cells Tissues Organs*, 141(1): 74-81.

MESTRES P, LÓPEZ-GÓMEZ L, NUÑEZ-LÓPEZ T, DEL ROSARIO G, LUKAS SW, HARTMANN U (2014) The basement membrane of the isolated rat colonic mucosa. A light, electron and atomic force microscopy study. *Ann Anat*, 196(2): 108-118.

MIRSADRAEE S, WILCOX HE, WATTERSON KG, KEARNEY JN, HUNT J, FISHER J, INGHAM E (2007) Biocompatibility of acellular human pericardium. *J Surg Res*, 143(2): 407-414.

NARAYANAN K, LECK KJ, GAO S, WAN AC (2009) Three-dimensional reconstituted scaffolds for tissue engineering. *Biomaterials*, 30(26): 4309-4317.

NICOSIA RF, OTTINETTI A (1990) Modulation of microvascular growth and morphogenesis by reconstituted basement membrane gel in three-dimensional cultures of rat aorta: a comparative study of angiogenesis in matrigel, collagen, fibrin, and plasma clot. *In Vitro Cell Dev Biol*, 26(2): 119-128.

OSAWA T, ONODERA M, FENG XY, NOZAKA Y (2003) Comparison of the thickness of basement membranes in various tissues of the rat. *J Electron Microsc*, 52(4): 435-440.

OZEKI M, NARITA Y, KAGAMI H, OHMIYA N, ITOH A, HIROOKA Y, NIWA Y, UEDA M, GOTO H (2006) Evaluation of decellularized esophagus as a scaffold for cultured esophageal epithelial cells. *J Biomed Mater Res A*, 79(4): 771-778.

PARSONS DS, PATERSON CR (1965) Fluid and solute transport across rat colonic mucosa. *Exp Physiol*, 50 (2): 220-231.

PATEL N, SOLANKI E, PICCIANI R, CAVETT V, CALDWELL-BUSBY JA, BHATTACHARYA SK (2008) Strategies to recover proteins from ocular tissues for proteomics. *Proteomics*, 8(5): 1055-1070.

PHILP D, CHEN SS, FITZGERALD W, ORENSTEIN J, MARGOLIS L, KLEINMAN HK (2005) Complex extracellular matrices promote tissue-specific stem cell differentiation. *Stem Cells*, 23(2): 288-296.

RANGAYYAN RM, KAMENETSKY I, BENEDIKTSSON H (2010) Segmentation and analysis of the glomerular basement membrane in renal biopsy samples using active contours: A pilot study. *J Digit Imaging*, 23(3): 323-331.

REING JE, BROWN BN, DALY KA, FREUND JM, GILBERT TW, HSIONG SX, BADYLAK SF (2010) The effects of processing methods upon mechanical and biologic properties of porcine dermal extracellular matrix scaffolds. *Biomaterials*, 31(33): 8626-8633.

REYNOLDS ES (1963) The use of lead citrate at high pH as an electron-opaque stain in electron microscopy. *J Cell Biol*, 17(1): 208-212.

RICCARDI C, NICOLETTI I (2006) Analysis of apoptosis by propidium iodide staining and flow cytometry. *Nat Protoc*, 1(3): 1458-1461.

RIEDER E, KASIMIR MT, SILBERHUMER G, SEEBACHER G, WOLNER E, SIMON P, WEIGEL G (2004) Decellularization protocols of porcine heart valves differ importantly in efficiency of cell removal and susceptibility of the matrix to recellularization with human vascular cells. *J Thorac Cardiovasc Surg*, 127 (2): 399-405.

SIMON-ASSMANN P, KEDINGER M (2000) Tissue recombinants to study extracellular matrix targeting to basement membranes. *Methods Mol Biol*, 139: 311-319.

SOTO-GUTIERREZ A, ZHANG L, MEDBERRY C, FUKUMITSU K, FAULK D, JIANG H, REING J, GRAMIGNOLI R, KOMORI J, ROSS M, NAGAYA M, LAGASSE E, STOLZ D, STROM SC, FOX IJ, BADYLAK SF (2011) A whole-organ regenerative medicine approach for liver replacement. *Tissue Eng Part C Methods*, 17(6): 677-686.

SPURR SJ, GIPSON IK (1985) Isolation of corneal epithelium with dispase-II or EDTA. Effects on basement membrane zone. *Invest Ophthalmol Vis Sci*, 26(6): 818 -827.

STANLEY BA, NEVEROVA I, BROWN HA, VAN EYK JE (2003) Optimizing protein solubility for two-dimensional gel electrophoresis analysis of human myocardium. *Proteomics*, 3(6): 815-820.

TIMPL R (1996) Macromolecular organization of basement membranes. *Curr Opin Cell Biol*, 8(5): 618-624.

WILLIAMSON JR, VOGLER NJ, KILO C (1969) Estimation of vascular basement membrane thickness: theoretical and practical considerations. *Diabetes*, 18(8): 567-578.

WILSHAW SP, KEARNEY JN, FISHER J, INGHAM E (2006) Production of an acellular amniotic membrane matrix for use in tissue engineering. *Tissue Eng*, 12(8): 2117-2129.

WU HS, DIKMAN S (2010) Segmentation and thickness measurement of glomerular basement membranes from electron microscopy images. *J Electron Microsc*, 59(5): 409-418.

YANG M, CHEN CZ, WANG XN, ZHU YB, GU YJ (2009) Favorable effects of the detergent and enzyme extraction method for preparing decellularized bovine pericardium scaffold for tissue engineered heart valves. *J Biomed Mater Res B Appl Biomater*, 91(1): 354-361.